

Influences of Rhyolitic Lava Flows on Hydrothermal Processes in Yellowstone Lake and on the Yellowstone Plateau

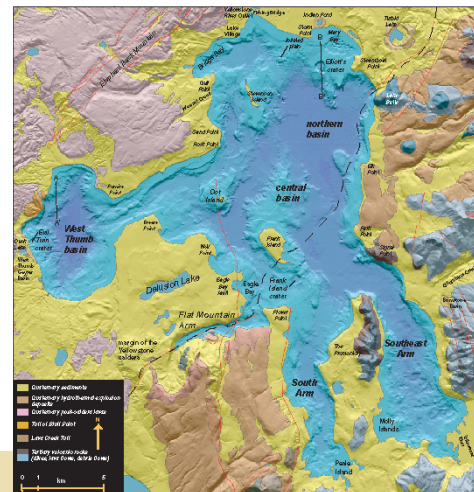


Lisa A. Morgan* | W.C. Pat Shanks III

U.S. Geological Survey

**Corresponding Author:*
U.S. Geological Survey
Denver Federal Center
Box 25046, MS 966
Denver, CO 80225-0046

Phone: 303.273.8646 Fax: 303.273.8600 Email: lmorgan@usgs.gov



ABSTRACT

Discoveries from multi-beam sonar mapping and seismic-reflection surveys of Yellowstone Lake provided new insight into the recent geologic forces that have shaped this large, high-altitude lake at the active front of the Yellowstone hot spot. The Yellowstone Plateau is strongly affected by young (<2 m.y.), large-volume (>7000 km³) silicic volcanism, active tectonism, and accompanying uplift. Mapping Yellowstone Lake has enhanced our understanding of the extent of postcaldera-collapse volcanism and active hydrothermal processes occurring above a large magma chamber not only in the lake but on the Yellowstone Plateau. Yellowstone Lake has an irregular bottom covered with dozens of features directly related to tectonic, volcanic, hydrothermal, glacial, and sedimentary processes that are similar to those observed on land within the Yellowstone Caldera. Detailed bathymetric, seismic-reflection, and magnetic evidence reveals that rhyolitic lava flows underlie much of Yellowstone Lake and exert fundamental control on lake morphology and localization of hydrothermal activity in the northern, West Thumb, and central lake basins. These observations have led us to investigate how on-land relationships influence the location of hydrothermal areas in the Yellowstone Caldera. We conclude the locations of many thermal features in the Yellowstone Caldera are directly influenced by the distribution of the rhyolitic lava flows.

Key Words

active deformation
hydrothermal processes
rhyolite
seasonal lake level variations
thermal disturbance
Yellowstone Lake
Yellowstone Plateau

1.0 INTRODUCTION

Yellowstone Lake straddles the southeast margin of the Yellowstone Caldera, and recent mapping efforts (Morgan et al. 2003) have revealed the geology of the lake basin. Yellowstone Lake is the centerpiece of the Yellowstone geocosystem, located in the heart of Yellowstone National Park (YNP) and surrounded by the steep Absaroka Range on its eastern and southeastern shores, and young rhyolite lava flows of the Yellowstone Plateau on its western and southwestern shores (**Figure 1**). Glacial, alluvial, and hydrothermal deposits are exposed around the margins of the lake.

Yellowstone Lake is the largest high-altitude lake in North America at an altitude of 2359 m (7733 ft) and a surface area of 341 km². More than 141 streams flow into the lake, 21 of which are significant in terms of their flow contribution. The Yellowstone River is the largest inflow and only outflow to the lake. The river enters at the south end of the Southeast Arm and drains north out of the lake at Fishing Bridge (**Figure 2, next page**) where discharge varied from 230–6720 cfs during the period from 1998–2004 (<http://nwis.waterdata.usgs.gov>).

From 1999–2003, the U.S. Geological Survey (USGS), in cooperation with YNP, mapped Yellowstone Lake (Morgan et al. 2003) utilizing state-of-the-art bathymetric, seismic, and submersible remotely operated vehicle (ROV) equipment. The new survey, navigated to an accuracy of <1 m using differential GPS, utilized more than 240 million soundings to produce the first high-resolution, continuous overlapping coverage of the lake bathymetry (**Figure 2**).

A significant result of the mapping effort is the recognition of post-caldera rhyolitic lava flows under a veneer of Holocene sediments

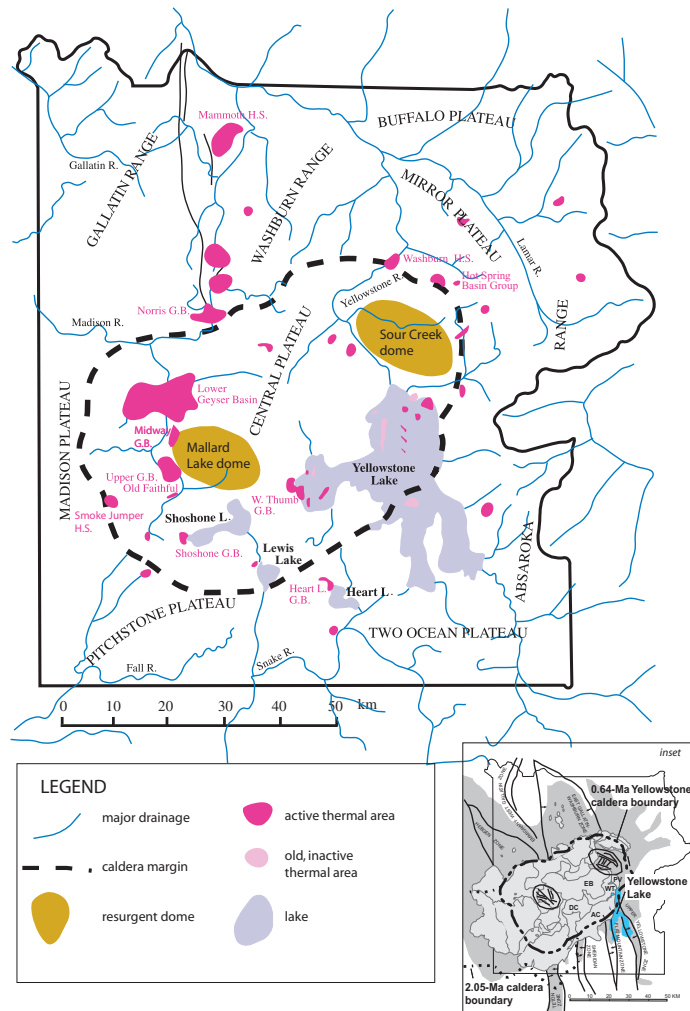
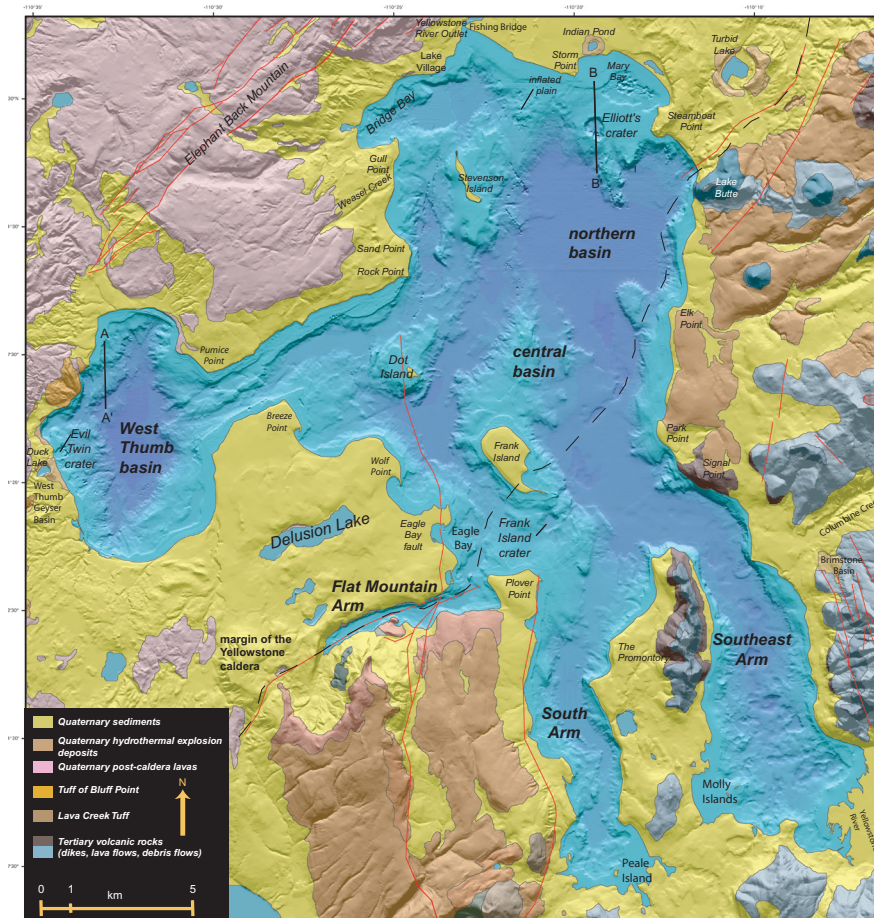


Figure 1. Index map showing the significant geologic features in YNP. Areas in red represent the primary locations of hydrothermal fields in the Park. In Yellowstone Lake, active thermal areas are shown in magenta; inactive are in pink.

Inset: Map of YNP (thin black line) showing the location of the Yellowstone Caldera (thick dashed line) in relation to its erupted product, the Lava Creek Tuff (shown in dark gray and distributed in a radial manner around the caldera), and post-caldera rhyolitic lava flows (shown in light gray; individual flow boundaries outlined in medium gray). The two resurgent domes and associated faults are shown in the center of the caldera as ovals with lines representing faults. The 2.05-Ma Huckleberry Ridge caldera is shown as a thick dotted line; the Yellowstone caldera overlaps its northeastern margin. Basin-and-Range structures are shown as thick black lines north and south of the Yellowstone caldera. The side of the line with the arrow on it represents the down-dropped side of the structure (modified from Hildreth et al. 1984). Yellowstone Lake is shown in blue. Rhyolitic lava flows noted include Pelican Valley (PV), Dry Creek (DC), Aster Creek (AC), West Thumb (WT), and Elephant Back (EB).



← **Figure 2. Blue-shaded high resolution bathymetric map of Yellowstone Lake** (modified from Morgan et al. 2003). Deeper shades of blue represent greater depths of water. The lake is surrounded by Tertiary Absaroka volcanic terrain to the southeast and east and by Quaternary post-caldera rhyolitic lava flows, sediments, and hydrothermal explosion craters (from USGS 1972). The line segment A-A' in West Thumb basin and B-B' in the northern basin are seismic reflection profiles shown in Figure 5. Red lines represent faults.

Figure 3 (at right). Preliminary geologic map of Yellowstone Lake (modified from Morgan et al. in press), **showing the main bedrock geology.** Units in lake are as shown in legend. Not shown on the geologic map is the mantle of glaciolacustrine deposits overlying most of the rhyolitic lava flows. The topographic boundary of the Yellowstone caldera cuts across the southern half of Frank Island and is shown as a thick dashed line.

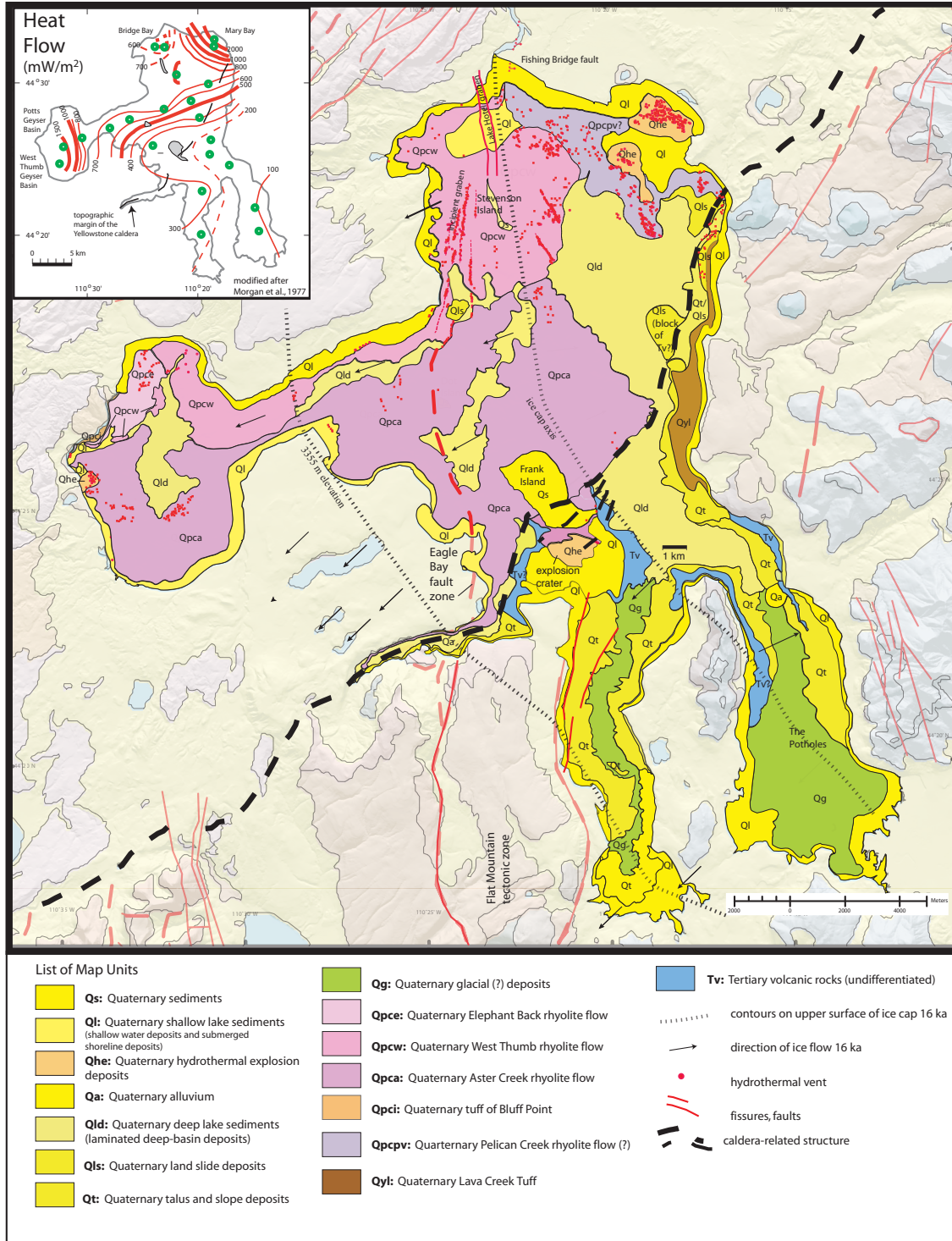
The thickest ice cap (>1 km) in the most recent glacial period resided in the central basin of Yellowstone Lake (Pierce 1979). Light dashed lines represent total elevation during the most recent glacial advance (Good and Pierce 1996). The maximum thickness of ice in Yellowstone Lake was in the central basin during the last glacial advance and is estimated to be >1 km thick, making the total elevation in the central basin ~16 ka in excess of 3355 m.

Glacial processes clearly overlapped volcanism, as evident in outcrop patterns present in the sublacustrine Aster Creek and West Thumb flows where the lavas may have been emplaced adjacent to large blocks of ice. The relatively flat sublacustrine plain near Bridge Bay in the northeastern part of the northern basin of the lake between lobes of the West Thumb flow and the adjacent Pelican Valley flow may have been occupied by a remnant block of ice; the thickest part of the Pinedale ice sheet is projected through this area (Good and Pierce 1996).

Likewise, large blocks of ice may have been present between flow lobes in the central basin when the Aster Creek flow was emplaced. The area around Yellowstone Lake is a shaded relief map with geology draped across it (modified from USGS 1972). Note the distribution of the rhyolitic lava flows surrounding the northern two-thirds of the lake.

Inset: Heat-flow values (in mW/m²) in Yellowstone Lake (modified after Morgan et al. 1977). Red lines represent thermal isograds; green circles represent heat flow sampling sites. Yellowstone Lake is outlined in gray; margin of Yellowstone Caldera shown as dashed line; Dot, Frank, and Stevenson Islands are shown in gray.

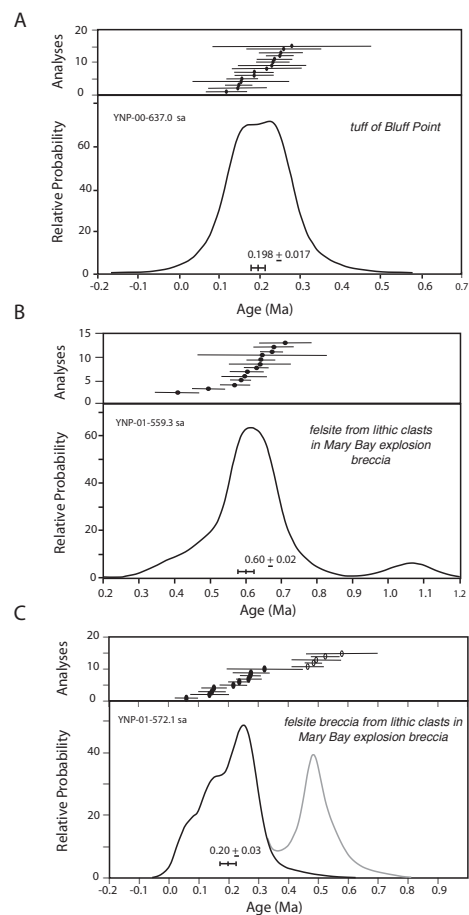
Figure 3. Preliminary geologic map of Yellowstone Lake



on the floor of the lake within the Yellowstone Caldera. The lava flows have a close spatial association with the location of hydrothermal vents (**Figure 3, previous page**). In this report, we discuss the influence of post-caldera rhyolitic lava flows in Yellowstone Lake on the distribution of hydrothermal features, and extend those observations onto land. In both environments, rhyolitic lava flows strongly influence the locations of hydrothermal systems by directing ascending hydrothermal fluids upward through fractured, permeable zones or laterally along permeable basal breccia zones to the periphery of lava flows.

2.0 GEOLOGIC SETTING

Powerful geologic processes in YNP produced the 75-km-by-45-km, 0.64-Ma Yellowstone Caldera (**Figures 1 and 2**; Christiansen 2001), one of the world's largest active silicic volcanoes (Mason et al. 2004). Yellowstone Lake, on the southeastern topographic margin of the Yellowstone Caldera, represents a somewhat obscure part of the caldera, where multiple geologic forces have contributed to the lake's form. Past volcanic events include the explosive caldera-forming 2.05-Ma eruption of the Huckleberry Ridge Tuff forming the Huckleberry Ridge caldera, followed by eruption of the 0.64-Ma Lava Creek Tuff to form the Yellowstone Caldera (**Figure 1 inset**; Christiansen 1984, 2001; Hildreth et al. 1984; Lanphere et al. 2002; USGS 1972). Following explosive, pyroclastic-dominated activity, two large resurgent domes were emplaced within ~100 ky after caldera collapse to the north and west of Yellowstone Lake. From 200 ka until ~70 ka, large-volume rhyolitic lava flows were emplaced in three pulses (Christiansen 2001) along the caldera margin, filling much of the caldera (**Figure 1 inset**). A smaller caldera-forming pyroclastic eruption, comparable in scale to Crater Lake, Oregon, occurred during the initial pulse creating the West Thumb caldera (Christiansen 1984; USGS 1972). Preliminary $^{40}\text{Ar}/^{39}\text{Ar}$ studies (McIntosh 2002, written communication) indicate that the eruption of the tuff of Bluff Point from the West Thumb caldera occurred at 198 ± 17 ka (**Figure 4A**), older than previously suggested based on K-Ar ages (161 ka; Christiansen 2001; Obradovich 1992).



↑ **Figure 4. Individual ages and age-probability distribution curves for single-crystal laser-fusion analyses for one sample from West Thumb basin and two samples from the lower Pelican Valley. A.** YNP-00-637.0: sanidine crystals from a vitrophyre in the tuff of Bluff Point in the West Thumb basin. **B.** YNP-01-559.3: sanidine crystals from felsite found as abundant lithic clasts in the Mary Bay explosion breccia in the lower Pelican Valley. **C.** YNP-01-572.1: sanidine crystals from a heterolithic breccia containing devitrified and silicified glassy felsites in the Mary Bay breccia. Upper panels show ages of individual analyses with 1-sigma error bars. Lower panels show age-probability distribution curves for each sample (W.C. McIntosh 2002, written communication). The younger age from YNP-01-572.1 is very similar to that of YNP-01-637.0, the tuff of Bluff Point, the ignimbrite erupted from the West Thumb caldera-forming event, at 0.198 Ma. These are preliminary ages and interpretations. Additional radiometric dating, paleomagnetic analyses, and mapping of these units are in progress.

Several significant glacial advances and recessions overlapped the volcanic events and had a strong effect on the shape of the Yellowstone Lake basin (Pierce 1974, 1979; Richmond 1976, 1977). Glacial scour deepened the central basin of the lake and the fault-bounded South and Southeast Arms (**Figures 1 inset and 2**). More recent dynamic processes shaping the lake include currently active fault systems and active deformation of the Yellowstone Caldera (Pelton and Smith 1982; Dzurisin et al. 1994; Wicks et al. 1998) recorded in a series of postglacial-shoreline terraces and young structural features (Hamilton 1987; Meyer and Locke 1986; Locke and Meyer 1994; Pierce et al. 2002). Finally, hydrothermal vents, craters, and domes, and large postglacial (<15 ka) hydrothermal-explosion craters, form the youngest features on the lake bottom.

2.1 Rhyolitic Lava Flows on the Yellowstone Plateau

The rhyolitic lava flows within the Yellowstone Caldera, known as the Central Plateau Member of the Plateau Rhyolite (Christiansen 2001), are very large and thick. Individual flows exceed 30 km in maximum dimension. Characteristic lava-flow morphologies include lobate forms, near-vertical margins (some as high as 300 m), rubbly vitric flow carapaces, hummocky or ridged tops, and strongly jointed interiors. Stream drainages tend to occur along flow boundaries rather than within flow interiors (Christiansen 2001; Christiansen and Blank 1975; USGS 1972). Many flows have vitrophyric exterior rinds with shrinkage cracks and sheet-jointed crystallized interior zones. Spherulitic and lithophysal zones commonly include large cavities. Breccias occur locally.

2.2 Rhyolitic Lava Flows in Yellowstone Lake

The discovery that rhyolitic lava flows underlie much of the lake floor north of and within the topographic margin of the Yellowstone Caldera (Morgan et al. 2003, and in press; **Figure 3**) allowed recognition that: (i) almost all of the Yellowstone Caldera is filled with rhyolitic lava flows, and (ii) many hydrothermal vents appear to be located preferentially along or close to the near-vertical edge of the lava flow. Seismic-reflection profiles in the near-shore areas of West Thumb basin show high-amplitude reflectors beneath about 7–10 m of layered lacustrine sediments

(**Figure 5A, next page**). We interpret these sublacustrine features as sediment-veneered rhyolitic lava flows (Morgan et al. 2003).

Subaerial lava flows including the Aster Creek, West Thumb, and Elephant Back flows can be traced into Yellowstone Lake by combining high-resolution bathymetric data with magnetic and seismic-reflection data (Morgan et al. 2003; Finn and Morgan 2002; **Figure 3**). The flows are defined by their general lobate plan-view form, hummocky flow tops and steep margins, and bulbous front scarps (**Figure 2**), despite being buried under 7–15 m of postglacial sediments. Based on available geochronology and field relationships, this series of lavas was erupted in the first pulse of post-200-ka eruptive activity within a short period—probably less than 10,000 years—of each other (Christiansen 2001).

A previously unmapped rhyolitic body is inferred at depth in the northern basin of Yellowstone Lake based on bathymetry and other data (Morgan et al. 2003; Finn and Morgan 2002). Clasts of hydrothermally altered, quartz-bearing felsite are prevalent in the hydrothermal-explosion breccia of Mary Bay and in the alluvium of the lower Pelican Valley (**Qpcpv, Figure 3**). The quartz-bearing felsite has not been identified before and is not a mapped unit in Christiansen (2001). Sanidine crystals from the felsite give a preliminary high-resolution $^{40}\text{Ar}/^{39}\text{Ar}$ age of 0.60 ± 0.02 Ma. Another clast from the Mary Bay breccia is a felsite breccia with two distinct well-grouped populations of sanidine crystals which may have been derived from different sources in the lower Pelican Valley: an older 500-ka rhyolite, and a younger 200-ka (0.200 ± 0.03 My) rhyolite (W.C. McIntosh 2002, written communication; **Figure 4B, C**). We suggest the felsite clasts are derived from either buried volcanic or shallow intrusive units beneath the lower Pelican Valley extending into the northern lake basin. Possibly two or more buried rhyolitic lava flows are present in lower Pelican Valley.

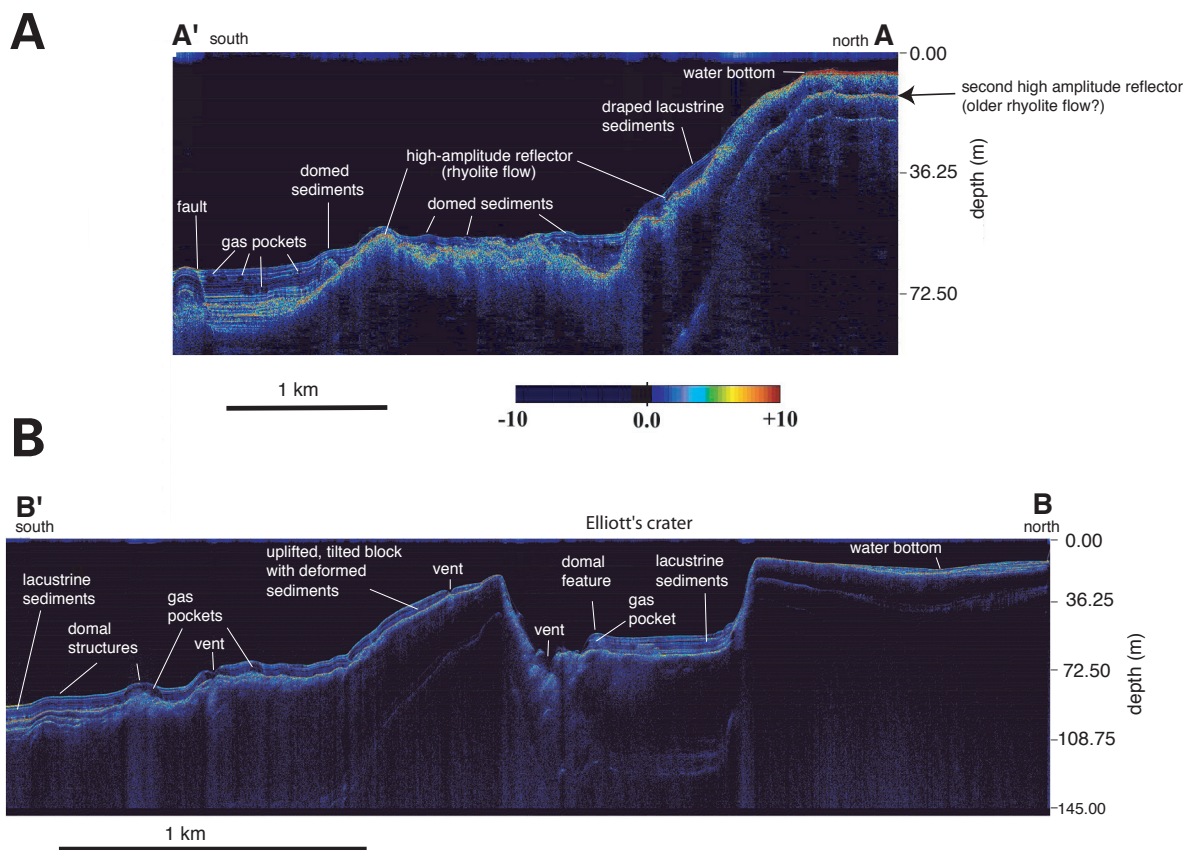
3.0 HYDROTHERMAL FEATURES

More than 650 active or recently active hydrothermal vent sites have been mapped in Yellowstone Lake (**Figure 3**).

Most occur in the northern and West Thumb basins although several thermal areas also are identified in the central basin (Figures 1, 2, and 3). These fields contain dozens of small hydrothermal vents in various stages of development and activity. In addition, four, and possibly seven, large hydrothermal explosion craters are present in the lake; within the craters are dozens of smaller active hydrothermal vents.

3.1 Formation of Hydrothermal Features

Formation of hydrothermal features in Yellowstone Lake is related to convective-meteoric hydrothermal-fluid circulation, steam separation during fluid ascent, and CO₂ accumulation and release above an actively degassing magma chamber. Hydrothermal explosions result from accumulation and sudden release of steam and/or CO₂—possibly reflecting changes in confining pressure that accompany, and may



↑ **Figure 5. A.** High-resolution seismic-reflection image from northwestern West Thumb basin showing a high-amplitude (discontinuous red and yellow) reflector interpreted as a sub-bottom rhyolitic lava flow. A second reflector beneath the primary reflector near the northern end of the profile may represent an older rhyolitic lava flow. Glacial and lacustrine sediments marked in blue overlie this unit. The profile A-A' is shown in Figure 2. The data amplitudes have been debiased and spatially equalized only; no additional gain corrections or filtering were applied.

B. High-resolution seismic-reflection image across part of Elliott's explosion crater showing small vents, gas pockets, and domed sediments in the lacustrine sediments that overlie the crater flank. The profile B-B' is shown in Figure 2. Lacustrine-sediment thickness in the main crater indicates 8-13 thousand years of deposition since the main explosion. More recent explosions, in the southern part of the large crater, ejected post-crater lacustrine sediments and created new and smaller craters. Colors are the same as for Figure 5A. Slightly modified from Morgan et al. (2003).

accelerate, failure and fragmentation of overlying rock. Sudden changes in pressure within the sealed hydrothermal system may be triggered by earthquakes, or in the case of submerged systems as in Yellowstone Lake, may be triggered by sudden changes in water level related to earthquakes, landslides, or other changes in the lake floor, such as collapse structures. Werner et al. (2000) and Werner and Brantley (2003) have shown that total CO₂ emissions in YNP approximate 45 kt/day. Sealing of surficial discharge conduits due to hydrothermal mineral precipitation contributes to overpressuring and may lead to sudden failure. Heat flow mapping (**Figure 3 inset**) shows that both the northern and West Thumb basins of Yellowstone Lake have extremely high heat flux (1650–15,600 mW/m²) compared to other areas in the lake (Morgan et al. 1977). Earthquake epicenter locations indicate that the areas within and surrounding the lake are seismically active (Smith 1991), and ROV studies identify hydrothermally active areas within the lake (Balistreri et al. in press; Klump et al. 1988; Remsen et al. 1990; Shanks et al. this volume).

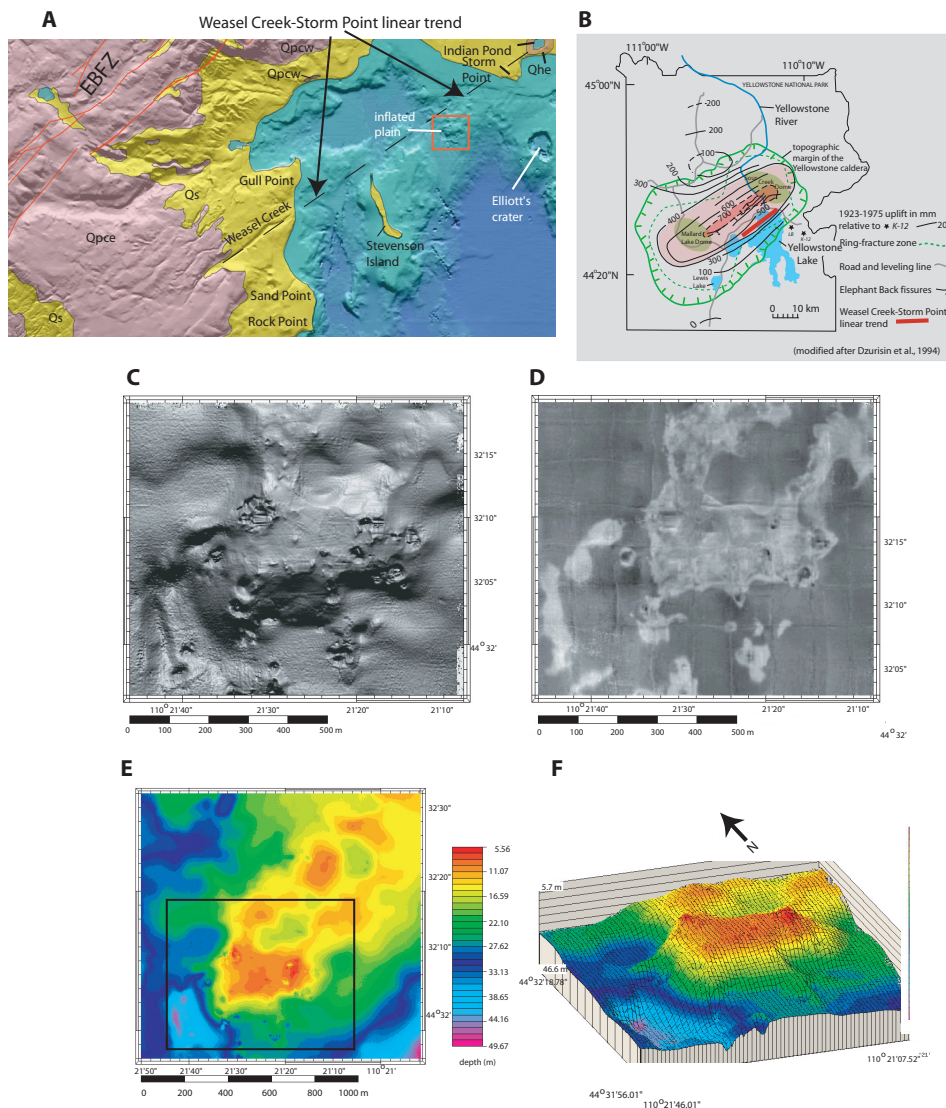
3.2 Characteristics of Sublacustrine Vent Sites

In seismic-reflection profiles (**Figure 5B**), hydrothermal vent features typically are imaged as V-shaped structures associated with reflective layers that are deformed or have sediments draped across their edges. Areas of high opacity (no discernable seismic reflections) occur directly beneath vent craters or in surrounding shallow sedimentary units. These opaque zones map subsurface gas pockets containing steam or CO₂, gas-charged fluids, or hydrothermally altered zones (Johnson et al. 2003). Evidence for lateral movement of hydrothermal fluids is seen beneath and adjacent to hydrothermal vents identified in the seismic-reflection profiles. Areas of opacity in the seismic data and zones of low values of magnetic intensity in the aeromagnetic data represent larger areas of hydrothermal alteration than those indicated by the surficial distribution of hydrothermal vents (Finn and Morgan 2002), and provide further evidence of lateral migration of hydrothermal fluids. Similar fluid migration northwest of the Yellowstone Caldera has been related by Waite and Smith (2002) to a localized 1985 earthquake swarm.

3.2.1 Fissures and faults. Hydrothermal vents are located along many structures identified in the recent mapping of

Yellowstone Lake and include large mapped faults and significant tectonic structures that continue onto land. North-trending faults from the Flat Mountain tectonic zone (**Figures 1 inset and 3**) enter the eastern bay of Flat Mountain Arm and continue northward as the young Eagle Bay fault (**Figure 3**). These faults include the hydrothermal vents north of Dot Island, a set of north-trending *en echelon* faults south of Rock Point identified in recent seismic reflection profiles, fissures west of Stevenson Island, and the Lake Hotel graben in the northern basin. All are oriented approximately north-south and probably are related to a regional structural feature in western Yellowstone Lake on strike with the Neogene Eagle Bay fault zone (Meyer and Locke 1986; Locke and Meyer 1994; Pierce et al. 1997; **Figure 3**). The set of fissures west and southwest of Stevenson Island are lined with mostly inactive hydrothermal vent sites and are extensional features; the fissures may represent an incipient graben that is offset from and forming to the southwest of the Lake Hotel graben. Northwest-trending fissures east of Stevenson Island host some of the deepest, hottest, and most active hydrothermal vents on the lake floor.

The sublacustrine fissures and faults are related to the regional tectonic framework of the northern Rocky Mountains and variable depths to the brittle-ductile transition zone (Fournier 1999) over the subcaldera magma chamber (Eaton et al. 1975; Fournier 1989; Fournier et al. 1976; Lehman et al. 1982; Stanley et al. 1991; Wicks et al. 1998). These structures play significant roles in shaping the morphology of the floor of Yellowstone Lake. Additionally, “breathing cycles” associated with the active and measured inflation and deflation of the Yellowstone Caldera create fissures or cracks along which hydrothermal fluids rise from depth. Most of these active deformation structures have prominent northeast and northwest trends reflecting the regional stress field that is associated with the young Yellowstone Caldera. As observed on land and in Yellowstone Lake, these structures act as conduits for ascending hydrothermal fluids and contribute significantly to the location of hydrothermal vents. Seismicity maps of the Yellowstone region (USGS Yellowstone Volcano Observatory Web site: <http://volcanoes.usgs.gov/yvo>) show concentrations of epicenters at various locations in Yellowstone Lake.



↑ **Figure 6.** A. High-resolution blue-shaded-relief bathymetric map of the northern basin of Yellowstone Lake highlighting the location of the inflated plain, Storm Point, Elliott's hydrothermal-explosion crater, the Elephant Back fissure zone (EBFZ), and the northeast-trending Weasel Creek-Storm Point linear trend. A geologic shaded-relief map of the area surrounds the lake (USGS 1972). Geologic units shown are in pink (Qpce=Quaternary Elephant Back flow, Qpcw=Quaternary West Thumb flow); yellow (Qs=Quaternary sediments); and tan (Qhe=Quaternary hydrothermal-explosion deposit). B. Simplified map of YNP highlighting location of the topographic margin of the Yellowstone Caldera, its two resurgent domes (Mallard Lake and Sour Creek), the Elephant Back fissures, and Yellowstone Lake. Superimposed on this, in black, are contour lines (in mm) showing the amount of total caldera uplift that occurred between 1923-1977 (modified from Dzurisin et al. 1994). The Weasel Creek-Storm Point linear trend is shown as a thick red line and coincides approximately with the 450 mm uplift contour interval. C. Gray-shaded-bathymetric close-up image of the inflated plain. Illumination is from due north with a sun-angle of 45°. D. Gray-scale backscatter-amplitude map of the same area shown in C. Bright areas are reflective due to their relative hardness and degree of silicification. Dark areas are sites of active hydrothermal vents. The range of reflectivity is from 26 to -20 dB. E. Two-dimensional color-bathymetric map of the inflated plain. Area shown in black box is the area shown in 6C and 6D. Total depth ranges from 5.56 to 49.76 m. F. Three-dimensional color-shaded-relief image of the inflated plain. Area shown is same as area in E but the image is rotated so that north is at 340° and is tilted 20°. Total depth ranges from 5.56 to 49.76 m. Data shown in A, C, D, E, and F are from 2002 mapping when this area was resurveyed.

3.2.2 Domes. Many vent areas are associated with small (1-10 m high) domal structures in which the original horizontally laminated, diatomaceous, lacustrine sediments have been arched upward (Johnson et al. 2003) by buoyantly ascending hydrothermal fluids that are generally rich in steam and CO₂. We infer that hydrothermal fluids permeate, silicify, and seal porous near-surface sediments resulting in development of an impermeable cap. The silicified cap sediments can be expected to compact less than unaltered muds surrounding the domes, which may contribute to the overall domal morphology. However, seismic reflection data (Otis and Smith 1977; Morgan et al. 2003; Johnson et al. 2003) indicate only 10-20 m of Holocene diatomaceous lake sediments. Assuming these post-glacial sediments are underlain by non-compactable, coarser-grained, glacio-lacustrine sediments or rhyolitic lava flows, then compaction is limited. Studies of marine sediments indicate that expected compaction of the upper 10 m of similar sediments is 10%-20% maximum, or 1-3 m (Breitzke 2000). Thus differential compaction may contribute to the relief of some smaller domes, but is unlikely to be a major part of the dome-forming process, especially for larger domes.

3.2.3 Large domes. Several large (10-40 m high; 500-1000 m diameter) hydrothermal domes have been recognized in the northern basin of Yellowstone Lake and are interpreted as structures associated with ascending hydrothermal fluids that have silicified and uplifted horizontally laminated sediments into domal forms (Johnson et al. 2003). These include the inflated plain, a large dome south of Stevenson Island off Sand Point, and Elliott's Crater, which shows evidence of doming prior to explosion. On land, Storm Point, a large 4-6-ka hydrothermal feature, shows evidence of doming in high-resolution LIDAR data (Pierce et al. 2002) and by diversion of stream channels away from these uplifted areas. Indian Pond may also have had a domal form prior to hydrothermal explosion, but definitive evidence is obscured by explosion breccia deposits.

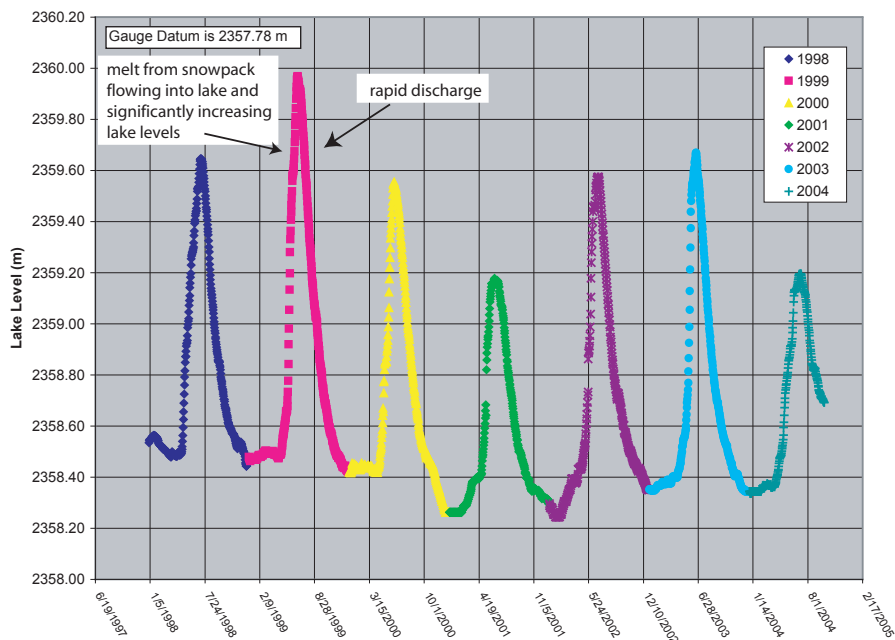
The most interesting northern lake domal structure, informally referred to as the inflated plain (**Figures 2 and 6**), was originally recognized in the 1999 bathymetric survey of the northern basin (Morgan et al. 1999) and was

resurveyed in 2002 to evaluate the possibility of presently active doming. The inflated plain covers an approximately circular area with a diameter of ~0.7 km, has a relatively flat top covered with smaller craters, and stands ~30 meters above the surrounding lake floor. Part of its relief may be due to its location within and along the edge of a rhyolitic lava flow (**Figures 2 and 3**); however, ROV observations show that laminated, silicified, and strongly jointed lake sediments from the inflated plain have steep dips. Seismic reflection data show that lake sediments on the edges of the structure also are dipping outward. Differential analysis of the 1999 bathymetric data with that collected in 2002 shows no measurable changes in the surface of the structure.

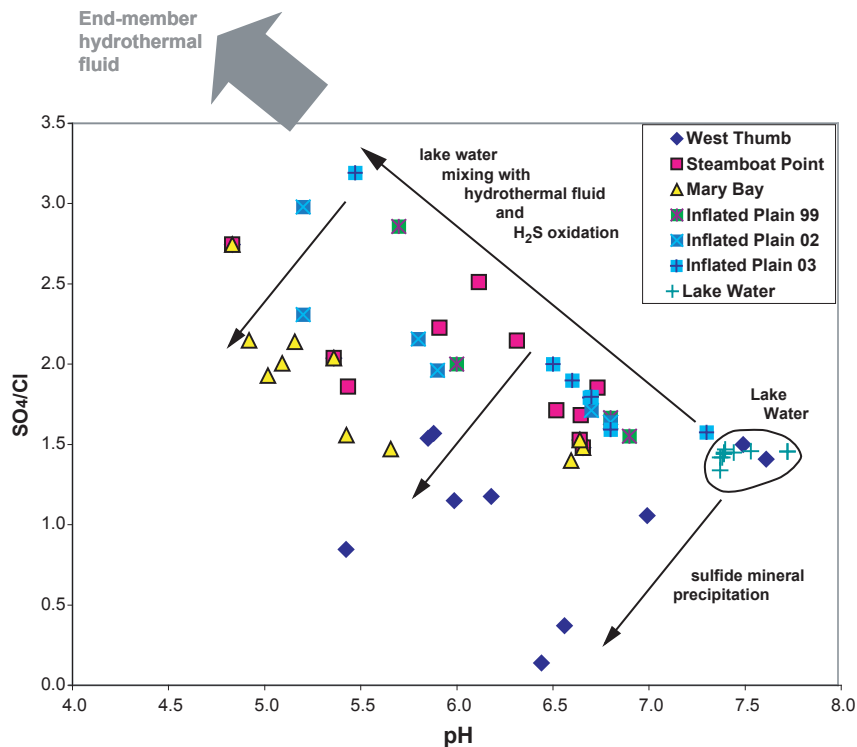
ROV exploration and high-resolution bathymetric images of the inflated plain (**Figure 6C**) show that the domal structure is pockmarked with numerous hydrothermal vents and craters. Clear evidence of hydrothermal alteration is seen in the sonar amplitude map (**Figure 6D**); bright areas are reflective due to their relative hardness. We infer that these brighter areas reflect higher degrees of silicification and may represent silicified caprock material, whereas the darker and less reflective areas are places where little silicification has occurred and active vents are concentrated. **Figures 6E and 6F** show the inflated plain in two- and three-dimensional perspectives and clearly demonstrate as much as 30 m of relief above the lake floor. Note smaller domal structures lie immediately northeast of the inflated plain in line with a fissure-like structure, similar and subparallel to those mapped on Elephant Back Mountain, informally referred to as the Weasel Creek-Storm Point linear trend (Morgan et al. in press).

As hydrothermal systems such as those on the inflated plain evolve, small and large domal structures may be preserved, may develop craters associated with hydrothermal explosions, or may be pocked with smaller craters that collapse below the sealed hydrothermal cap due to hydrothermal dissolution of the underlying sediment (Shanks et al. this volume).

3.2.4 Effects of seasonal lake level variations on hydrothermal venting. In late September 2002, while



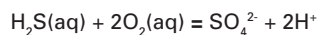
← **Figure 7.** Lake level data and discharge data for the U.S. Geological Survey Fishing Bridge gauging station, downloaded from the National Water Information System (NWIS, http://nwis.waterdata.usgs.gov/wy/nwis/discharge/?site_no=06186500), were fit to a power series regression, enabling calculation of lake level data from the daily discharge data available for the period 1998-2004.



← **Figure 8.** SO₄/Cl plotted against pH for hydrothermal fluids sampled from sublacustrine vents in Yellowstone Lake between 1996-2003. Fluid samples collected at the inflated plain between 1999-2003 show no significant change in chemistry over the 4-year period, except that 3 of the 2002 samples show stronger lower pH, perhaps due to entrainment of acid-sulfate fluids during a sublacustrine "fall disturbance".

traversing the area over the inflated plain in the RV Cutthroat, we noted several unusual phenomena not observed in our previous surveys conducted in late June and July. Phenomena included a strong scent of H₂S, a 30- to 50-m-diameter plume of fine sediments, and large concentrations of rising bubbles, many of them quite vigorous. The fine-sediment plume was first detected by the Fathometer as a strong “false bottom” reflector at ~3 m below the lake surface, and was later confirmed to originate from a sediment plume in the water column. Submersible dives to the lake floor at 15-25 m depth in this area confirmed the nature of the mid-water column reflector. We have reoccupied this site in subsequent years (2003, 2004) and note that the phenomena observed in late summer 2002 are not apparent in the early summer, but were observed in mid-to-late August 2004, which was a low water year compared to 2002 (**Figure 7**). This timing coincides with changes in lake levels which are high in June and July and quickly drop off by 25-50 cm in late August and September (**Figure 7**).

In order to evaluate these variations in hydrothermal activity, fluids were collected from active vents on the inflated plain from 1999, 2002, and 2003, and analyses showed no dramatic change in chemistry over this four-year period (**Figure 8**). Because hydrothermal Cl⁻ and H₂S-rich vent fluids mix with cold dilute, oxygenated lake waters that circulate in shallow sediments, fluid mixing results in dilution and oxidation even before fluids vent on the lake bottom (Balistrieri et al. in press; Shanks et al. this volume). To understand the bulk chemistry of such rapidly evolving fluids, the ratio of SO₄ to Cl is plotted in **Figure 8** to account for variable dilution of individual samples. In addition, H₂S oxidation affects vent fluid pH by creating acid, as follows:



Thus, arrays on SO₄/Cl vs. pH plots account for the bulk composition of venting fluids, and the similar arrays for different sample years on the inflated plain (**Figure 8**) suggest little or no fundamental change to the hydrothermal system.

We attribute the observed phenomena in late summer and fall as being associated with a drop in lake level

significant enough to lower the hydrostatic head on active hydrothermal vent systems. On the inflated plain, this results in release of H₂S-rich gas bubbles and entrainment of fine-grained sediments in the upwelling hydrothermal vent fluids. Based on field observations from 1999-2004 and on annual lake level curves (**Figure 7**), it seems likely that the seasonal phenomena described for late summer/fall are typical and do not represent an intensification of hydrothermal activity.

At Norris Geyser Basin, Fournier et al. (2002) documented potential causes of the long observed “fall disturbance” that produces sudden changes in some thermal springs at Norris, including turbid, sediment-rich fluids; sudden fluctuations in temperature and steam generation; and variations in pH, SO₄, and Cl that indicate mixing with shallow acid-sulfate waters. Fournier et al. (2002) suggest that the fall disturbance is due to a slight but critical drop in water table that lowers pressure to a point where fluids flash to steam in shallow subsurface parts of the system. Because wall rocks are also hot, and do not adjust to temperature as rapidly as the fluids, this leads to strongly fluctuating systems and entrained waters from shallow parts of the reservoir. Turbidity is inferred to come from clays produced in acid-sulfate alteration zones. These conclusions, if applicable to the inflated plain, imply that there may be a zone of acid sulfate waters in the shallow subsurface there.

3.2.5 Large hydrothermal explosion craters. Large hydrothermal explosion craters in Yellowstone Lake include the (4-6 ka) Evil Twin explosion crater in western West Thumb basin, the greater-than-10-ka Frank Island crater in the south central basin, and in the northern basin, the 13- to 8-ka Elliott’s crater (Johnson et al. 2003) and the 13.6-ka Mary Bay explosion crater (Pierce et al. 2002; Wold et al. 1977; Morgan et al. 2003; **Figure 2**). All have nested craters indicative of multiple cratering events over a period of time, perhaps thousands of years. Many of the smaller craters within the parent crater may have formed from a variety of processes, including not only hydrothermal explosions but also collapse associated with dissolution of lake muds (Shanks et al. this volume).

All identified large explosion craters in Yellowstone Lake, except for the Frank Island crater, have active hydrothermal vents (Morgan et al. 2003); emit relatively high-temperature hydrothermal fluids (Balistrieri et al. in press; Shanks et al. this volume) ranging from 72°C in West Thumb to $\geq 95^\circ\text{C}$ at Mary Bay (Gemery-Hill et al. in press); and are located within or near the edges of post-caldera rhyolitic lava flows (**Figure 3**). The Frank Island hydrothermal explosion crater and three other possible explosion craters east of Frank Island lie along the topographic margin of the Yellowstone Caldera, as do similar on-land explosion craters (Muffler et al. 1971; Richmond 1973; Morgan et al. 1998) such as the 8.6-ka Turbid Lake and Fern Lake craters. The Fern Lake explosion crater also is adjacent to the northeast edge of Sour Creek resurgent dome. Other large hydrothermal features, such as the Indian Pond, Duck Lake, and Mary Bay explosion craters, and large hydrothermal domes at Storm Point and inflated plain, are located at the edges (Duck Lake) or within rhyolitic lava flows, and are focused along northeast-trending structures, subparallel to northeast-trending fissures on Elephant Back Mountain, and associated with deformation of the Yellowstone Caldera (**Figure 6A, B**).

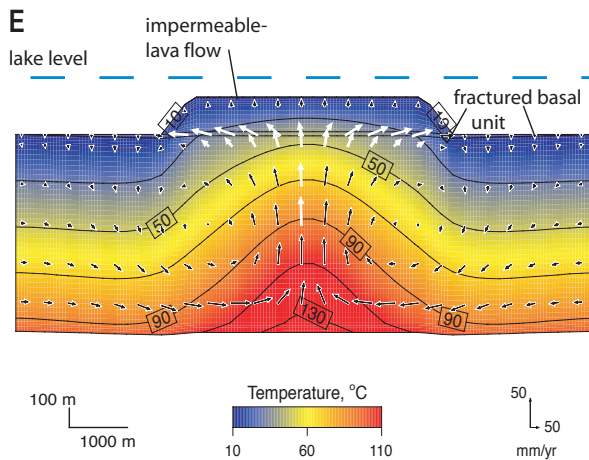
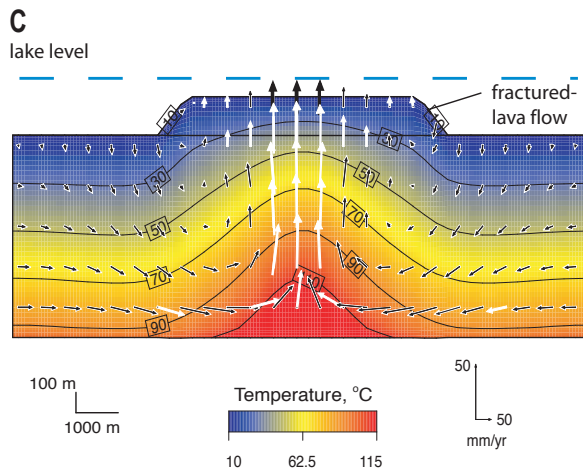
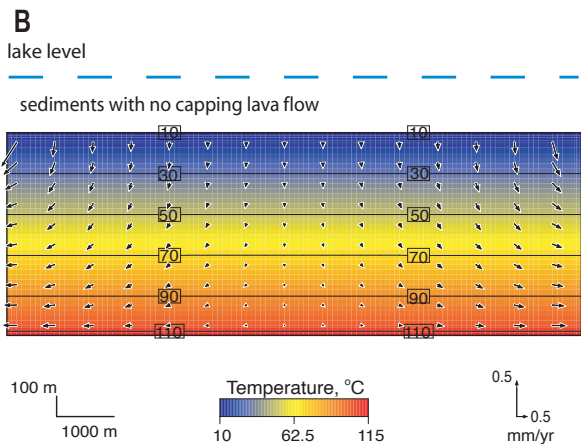
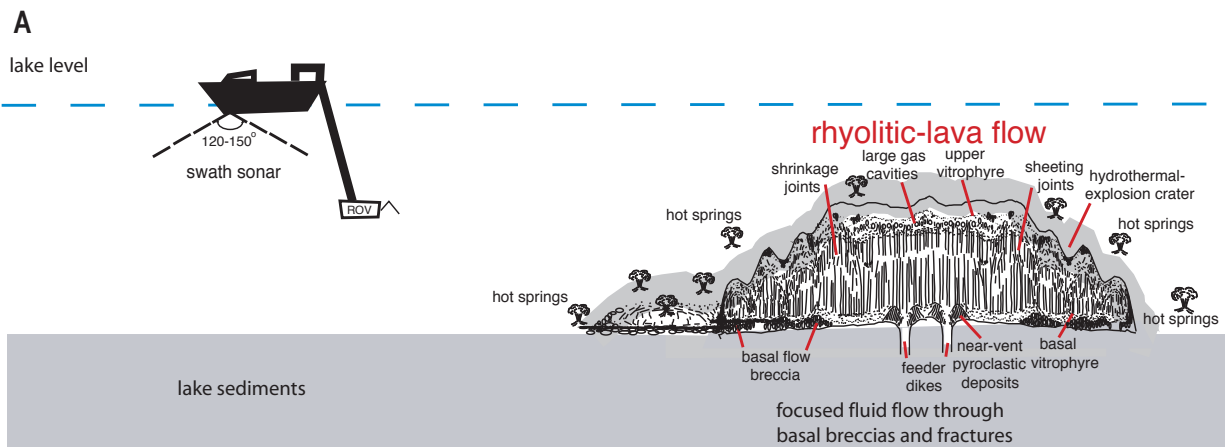
4.0 HYDROTHERMAL FEATURES ON THE YELLOWSTONE PLATEAU

Hydrothermal activity in YNP is concentrated within the Yellowstone Caldera although additional thermal areas also are found outside the caldera along major tectonic zones, especially the north-trending Norris-Mammoth fault zone. Hydrothermal activity has been intensive for the past 15 ky (Fournier 1999), and U-series ages of travertine deposits near Mammoth indicate significant periods of deposition at about 375, 134, 50, 20, and 15 ka to present (Sturchio et al. 1991, 1994).

The locations of several thermal areas in YNP as plotted in **Figure 9** on geologic maps clearly show their relation to various structures and geologic units, especially rhyolitic lava flows (modified after Christiansen 2001). Significant features where hydrothermal systems are located include tectonic zones outside the Yellowstone Caldera, the topographic margin of the Yellowstone Caldera, areas within the Yellowstone Caldera at the edges of rhyolitic lava flows, and faults or extensional fissures associated with active deformation of the Yellowstone Caldera. Previous interpretations of controls for some hydrothermal features located within the Yellowstone Caldera relate these to an inferred ring-fracture zone (Christiansen 2001).

← **Figure 9. Geologic maps highlighting the locations of thermal areas in relation to various structures and deposits in YNP** (modified after Christiansen 2001 and U.S.G.S. 1972). **A.** Geologic map showing hydrothermal vent and thermal area distribution in the northern Park along the northern margin of the Yellowstone Caldera and the Norris-Mammoth tectonic corridor. **B.** Geologic map showing hydrothermal vent and thermal area distribution in the western Park along the southwestern margin of the Yellowstone Caldera and includes thermal areas at the Lower, Midway, Upper, Shoshone, and West Thumb Geyser Basins. Yellowstone Lake is shown on the right, with thermal areas in red.

Features are represented as: the Yellowstone Caldera (thick dashed black line); Norris-Mammoth tectonic corridor (thinner dashed black lines); faults or fissures at Sour Creek dome, Mallard Lake dome, and Elephant Back Mountain (thin black lines); thermal areas (in red). The locations of individual hydrothermal vents determined by differential GPS (A. Rodman 2005, written communication) are plotted in green and represent data collected up to the summer of 2005; this is a work in progress. Yellow stars are shown to represent individual lava flow eruptive vents at the Mary Mountain flow and Nez Perce flow (Figure 9A), and Summit Lake flow (Figure 9B). Units in pink, outlined in gray, represent Quaternary Central Plateau post-caldera rhyolitic lava flows and include Qpcy (West Yellowstone flow), Qpcn (Nez Perce flow), Qpcm (Mary Lake flow), Qpcf (Solfatar Plateau flow), Qpch (Hayden Valley flow), Qpcu (Spruce Creek flow), Qpce (Elephant Back flow), Qpcw (West Thumb flow), Qpcs (Summit Lake flow), Qpcr (Bechler River flow), Qpcb (Buffalo Lake flow), Qpca (Aster Creek flow), Qpcc (Spring Creek flow), Qpcd (Dry Creek flow), Qpci (tuff of Bluff Point), and Qpco (tuff of Cold Mountain Creek). Units in tan are rhyolites Quaternary Upper Basin post-caldera rhyolitic lava flows and include Qpuc (Canyon flow) and Qpul (Scaup Lake flow). Unit in medium pink in Figure 9B is the rhyolite of the Mallard Lake Member of Plateau Rhyolite, Qpm (Mallard Lake flow). Units in dark pink in Figure 9A on the edge and north of the Yellowstone caldera are post-caldera rhyolitic lavas and include Qprg (Gibbon River flow) and Qpro (Obsidian Creek flow). Other geologic units on map but not individually labeled include the Quaternary Lava Creek Tuff (light green), Quaternary basalt lava flows (medium green and green with red v's), Quaternary sediments (yellow), Tertiary volcanic rocks (light and dark blue), Precambrian rocks (brown), and Tertiary-Mesozoic-Paleozoic rocks (dark olive and blue).



However, geological and geophysical evidence shows that many hydrothermal vent fields are located at the edge of rhyolitic lava flows. In addition, some vents are located at the edge of lavas along young exposed faults formed by the inflation–deflation cycles of the Yellowstone Caldera (Dzurisin et al. 1994; Pelton and Smith 1982; Pierce et al. 2002).

The combination of high heat flow and tectonic fractures at depth contributes significantly to the general location of hydrothermal features (Christiansen 2001). These major tectonic features are expressed most obviously as north-trending zones of normal faulting that extend south of the caldera eastward from the Teton Fault to the Heart Lake area and north of the caldera along the Norris–Mammoth corridor. These fault zones obviously exert a strong influence on localization of major hydrothermal basins at Heart Lake, Monument Geyser Basin, Roaring Mountain, and Mammoth Geyser Basin. Norris Geyser Basin is located at the intersection of the Norris–Mammoth corridor and the northwestern margin of the Yellowstone Caldera.

Several prominent thermal areas are mapped along the topographic margins of both the Huckleberry Ridge and Yellowstone Calderas. **Figure 9B** shows thermal areas along the Snake River and Red Mountains caldera segments of the 2.05-Ma Huckleberry Ridge caldera in the southeastern part of the Park. Heart Lake Geyser Basin is located at the intersection of caldera-related structures of the Red Mountains segment, the younger Yellowstone Caldera margin, and north-trending normal faults. Clearly, deep-seated structures form conduits for ascending hydrothermal fluids at these locations.

The influence of the topographic margin of the Yellowstone Caldera on thermal vents locations can be further demonstrated at Hot Springs Basin Group, Washburn, Joseph’s Coat, Whistler, Mushpots, Astringent Creek, and Porcupine Hot Springs basins (**Figure 9A**). Terrace Hot Springs, along the northwestern margin of the Yellowstone Caldera, occurs at the intersection of the caldera margin and a set of northwest-trending faults outside the caldera. Smoke Jumper Hot Springs is one of the few thermal areas along the southwestern margin of the Yellowstone Caldera; here it is in the middle and top of the Summit Lake rhyolite flow. The vent area for the Summit Lake flow is mapped at Smoke Jumper Hot Springs (Christiansen 2001) and may have contributed to the location of the hot springs by ascending hydrothermal fluids through fractured eruptive vent rocks.

Within the Yellowstone Caldera, the post-caldera Central Plateau Member of the Plateau Rhyolite consists of about 21 rhyolites—the majority of which are lava flows—which now occupy the topographic depression of the caldera. New mapping of individual hydrothermal vent areas using differential GPS (A. Rodman 2005, personal communication) clearly demonstrates the close spatial relationship of thermal vents to rhyolitic lava flows. The Mud Pots, Black Dragon, and Mud Geysers thermal areas occur at the intersection of northwest-trending faults associated with the Sour Creek dome, the northeast-trending fissures on Elephant Back Mountain, and the edges of the West Thumb (**Qpcw**), Elephant Back (**Qpce**), and Hayden Valley (**Qpch**) rhyolitic lava flows (**Figure 9**).

← **Figure 10.** **A.** Schematic diagram showing physical features of a rhyolitic lava flow (modified from Bonnicksen and Kauffman 1987). **B.** Two-dimensional fluid-flow model with simple glaciolacustrine-sedimentary aquifer (no caprock) that results in low flow velocities, recharge at the surface, and lateral flow out of both ends of the model aquifer. Subsurface temperatures never exceed 114°C, as indicated by contours and color map. Fluid-flow rates are low (<0.7 mm/yr) as indicated by velocity vectors. **C.** Fluid-flow model with a fully cooled rhyolitic lava flow acting as caprock. The underlying sedimentary aquifer and heat flow are the same as in the previous model. The addition of a 200-m-thick fractured crystalline-rock cap strongly focuses the upward limb of an intense convection cell under the caprock. In this model, fluid temperatures reach 140°C and flow velocities are as high as 150 mm/yr. **D.** Photograph of the edge of rhyolitic lava flow. Note the abundance of thermal features at the base and edge of the flow. **E.** Fluid-flow model that includes a basal breccia zone beneath an impermeable lava flow. In this case, the lower sedimentary unit is overlain by a thin, fractured, lava-flow unit (20 m thick) that extends the entire width of the sedimentary prism. Above the more permeable basal unit is a 170-m-thick low-permeability unfractured lava flow. Flow vectors indicate strong upflow under the lava flow with maximum subsurface temperatures of ~150°C and flow rates up to 160 mm/yr. Upflow is deflected laterally within the 20-m-thick “basal” fractured zone toward the flow edges, resulting in hydrothermal venting on the lake floor near the margins of lava flows.

In the Lower and Upper Geyser Basins and surrounding areas, thermal areas clearly are close to the edges of individual rhyolitic lava flows and/or at the contact where two or more lava flows abut each other with small sediment-filled alluvial basins between the flows. The older Nez Perce (160 ± 2 ka, Obradovich 1992) and Elephant Back (153 ± 2 ka, Obradovich 1992) flows most likely extend out into the Lower Geyser Basin and are overlain by sediment fill. The younger West Yellowstone flow (108 ± 1 ka; Obradovich 1992) filled the area west of these older flows. Individual vent locations in the Midway Geyser Basin, many aligned along northwest trends, are clearly influenced by the northwest-trending faults and structures associated with the northwest edge of Mallard Lake resurgent dome, also a post-caldera rhyolitic lava flow (**Figure 9B**). In the Upper Geyser Basins, individual hydrothermal vents mark the edge of the Mallard Lake flow.

5.0 DISCUSSION

A basic observation from our lake surveys is the close spatial relationship that exists between the distribution of hydrothermal areas and sublacustrine rhyolitic lava flows (Morgan et al. in press). Not only does this observation hold true for many of the vents in Yellowstone Lake but also appears to hold on land for many thermal areas within the caldera. Spatial and field data indicate that the majority of thermal areas in the subaerial portion of the Yellowstone Caldera, where post-caldera rhyolitic lava flows have filled the caldera (**Figure 1 inset**), are located along the edges of flows (**Figure 9**). Rhyolitic lava flows and structures exposed at the surface control the location of a majority of hydrothermal areas within the caldera and have a profound influence on the flow of shallow groundwater. This interpretation is a refinement of the view that the locations of past and current hydrothermal fields are strictly controlled by deep-seated structures.

The Yellowstone Caldera, which includes the northern two-thirds of Yellowstone Lake, lies above a large magma chamber that may be periodically replenished (Eaton et al. 1975; Fournier 1989, 1999; Fournier et al. 1976; Lehman et al. 1982; Stanley et al. 1991; Wicks et al. 1998; Christiansen 2001). The close relationship between

hydrothermal features and the edges of rhyolitic lava flows can be seen in **Figures 3 and 9**.

Based on our observations of the abundant present-day distribution of hydrothermal vents, Morgan et al. (2003) developed a flow model for sublacustrine conditions that predicts that fully cooled, rhyolitic lava flows exert a fundamental influence on subsurface hydrology and hydrothermal-vent locations (**Figure 10**). Upwelling hydrothermal fluids are focused at depth along pre-existing faults and fractures and, as they near the surface, fluids migrating from these conduits are focused preferentially through the fractured edges of rhyolitic lava flows (**Figure 10E**) or into enclosed, more permeable basins surrounded by lavas yet still profoundly affected by presence of the lava flows. In contrast, hydrothermal fluids flowing through lake and glacial sediments tend to be more diffuse (**Figure 10B**).

In the subaerial environment, our fluid flow model (Morgan et al. 2003) is rigorously applicable only in the saturated zone below the water table, but assuming much of the volume of subaerial lava flows on the Yellowstone Plateau is below water table, our conclusions stand. Certainly, the same spatial relations are observed in both subaerial and sublacustrine environments where the locations of hydrothermal vents or thermal fields appear to be focused near the edge of rhyolitic lava flows (**Figures 9 and 10**). In both environments, convective flow moves laterally through basal flow breccias away from thicker, more impermeable segments of the rhyolite flow toward the fractured-flow margin, where the majority of hydrothermal activity is observed (**Figure 10E**).

As previously proposed (Christiansen 2001), pre-existing north-south-trending structures associated with older Basin-and-Range structures once extended across the pre-caldera terrain of the Yellowstone Caldera (**Figure 1 inset**). These continue to exert an influence at depth for fracture-controlled flow and distribution of hydrothermal features; however, this is most common outside the caldera (**Figure 9A**). For the area within the caldera, now almost completely filled with large viscous rhyolitic lava flows (**Figure 1 inset**), fluids ascend along deep faults and

fissures. Located above these structures, thick rhyolitic lava flows above permeable basal breccias and sediments exert a strong influence on the fluid flow dynamics in the shallow subsurface and control the location of many present-day hydrothermal vents.

Most water responsible for recharging the hydrothermal systems in Yellowstone is meteoric; oxygen and hydrogen isotopes indicate that >70–85% of the water is derived from snowpack (Rye and Truesdell 1993; Fournier 1999). The Yellowstone Plateau is a broad high terrain that receives more than 180 cm of precipitation each year from wet, northeast-moving weather systems. The abrupt increase in elevation of approximately 1 km from the eastern Snake River Plain northeast to the Yellowstone Plateau is responsible for the rapid and heavy precipitation on the plateau (Pierce et al. in press). Poor drainage off the high plateau surfaces of individual rhyolitic lava flows is reflective of the generally impermeable interior of massive rhyolitic lava flows. Dobson et al. (2003) have shown that both Lava Creek Tuff and a Central Plateau rhyolitic lava flow are essentially impermeable units with measured permeabilities that average 0.1 millidarcy. Where fractured, both of these lithologies show local higher permeability zones that may transmit hydrothermal fluids, which may account for hydrothermal areas like Smoke Jumper Hot Springs located in the interior of lava flows.

Results of our model (Morgan et al. 2003; **Figure 10E**) indicate strong convective upflow under the lava flow, with maximum subsurface temperatures of 150°C and flow rates as much as 160 mm/yr. As expected, upflow is strongly influenced by the overlying low-permeability of the unfractured lava flow and is deflected laterally to the edges of the flow. Lateral flow proceeds within a 20-m-thick “basal” fractured zone away from the central upwelling zone toward the flow edges on either side, resulting in hydrothermal venting near the margins of lava flows. This physical model explains the preferential distribution of hydrothermal vents near or at the edges of rhyolitic lava flows on the Yellowstone Plateau (**Figure 10A**).

6.0 CONCLUSIONS

Yellowstone Lake is unique in being one of the most significant hydrothermal areas in YNP and being the only one of its size completely submerged under water. Geochemical studies of sublacustrine vents in Yellowstone Lake indicate that ~10% of the total deep-thermal-water flux in YNP occurs on the lake bottom (Balistrieri et al. in press; Shanks et al. this volume). Mapping Yellowstone Lake has enhanced our understanding of hydrothermal processes within and along the margins of the Yellowstone Caldera.

While deep structures (Christiansen 2001) and ongoing deformation of the Yellowstone Caldera continue to exert important controls on many structures within the caldera that provide conduits for ascending hydrothermal fluids, the strong influences exerted by overlying rhyolitic lava flows on the location of hydrothermal areas should not be overlooked. As our mapping, observations, and flow model demonstrate, shallow subsurface hydrologic processes are strongly influenced by the landscape of rhyolitic lava flows within the Yellowstone Caldera and require that more than deep structural controls are responsible for locations of hydrothermal features present within the Yellowstone Caldera.

ACKNOWLEDGEMENTS

We acknowledge and thank Bill McIntosh for the preliminary radiometric analyses presented herein, and Boris Schulze and Ron Sweeney for their contributions on various maps. We thank David Lovalvo of Eastern Oceanics, Inc. for ROV studies and for coordinating our field studies in Yellowstone Lake. We also thank Laurie Wirt, Jacob Lowenstern, and Bill Inskeep for their thorough and helpful reviews. We are grateful to Ann Rodman and Carrie Guiles at the Yellowstone Center for Resources (YNP) for the differential GPS data on individual hydrothermal vents and thermal areas in the Park, and acknowledge the detailed and difficult efforts made in creating such a thorough data set. We also thank Susan Kelly and Martha Sellers for their edits and assistance.

REFERENCES

- Balistreri, L.S., W.C. Shanks, III, R.L. Cuhel, C. Aguilar, and J.V. Klump. In press, The influence of sublacustrine hydrothermal vents on the geochemistry of Yellowstone Lake. In *Integrated Geoscience Studies in the Greater Yellowstone Area: Volcanic, Hydrothermal, and Tectonic Processes in the Yellowstone Geocosystem*, ed. L.A. Morgan. US Geol Surv Prof Pap.
- Bonnichsen, B., and D.F. Kauffman. 1987. Physical features of rhyolite lava flows in the Snake River Plain volcanic province, southwestern Idaho. In *The emplacement of silicic domes and lava flows*, ed. J.H. Fink, 119–45. Geol Soc Am Special Paper 212.
- Breitzke, M. 2000. Physical properties of marine sediments. In *Marine Geochemistry*, ed. H.D. Shulz and M. Zabel. Berlin-Heidelberg: Springer Verlag.
- Christiansen, R.L. 1984. Yellowstone magmatic evolution—Its bearing on understanding large-volume explosive volcanism. In *Explosive volcanism—Inception, evolution, and hazards*, 84–95. Washington, DC: National Academy Press.
- Christiansen, R.L. 2001. The Quaternary and Pliocene Yellowstone Plateau volcanic field of Wyoming, Idaho, and Montana. *US Geol Surv Prof Pap* 729-G.
- Christiansen, R.L., and H.R. Blank, Jr. 1975. Geologic map of the Canyon Village quadrangle, Yellowstone National Park, Wyoming. *US Geol Surv Geol Quad Map* GQ-1192.
- Dobson, P.F., T.J. Kneafsey, J. Hulen, and A. Simmons. 2003. Porosity, permeability, and fluid flow in the Yellowstone geothermal system. *J Volcanol Geotherm Res* 123:313–24.
- Dzurisin, D., K.M. Yamashita, and J.W. Kleinman. 1994. Mechanisms of crustal uplift and subsidence at the Yellowstone caldera, Wyoming. *Bull Volcanol* 56:261–70.
- Eaton, G.P., R.L. Christiansen, H.M. Iyer, A.M. Pitt, D.R. Mabey, H.R. Blank, Jr., I. Zietz, and M.E. Gettings. 1975. Magma beneath Yellowstone National Park. *Science* 188:787–96.
- Finn, C.A., and L.A. Morgan. 2002. High-resolution aeromagnetic mapping of volcanic terrain, Yellowstone National Park. *J Volcanol Geotherm Res* 115:207–31.
- Fournier, R.O. 1989. Geochemistry and dynamics of the Yellowstone National Park hydrothermal system. *Ann Rev Earth Planet Sci* 17:13–53.
- Fournier, R.O. 1999. Hydrothermal processes related to movement of fluid from plastic into brittle rock in the magmatic-epithermal environment. *Econ Geol* 94:1193–1212.
- Fournier, R.O., U. Weltman, D. Counce, L.D. White, and C.J. Janik. 2002. Results of weekly chemical and isotopic monitoring of selected springs in Norris Geyser Basin, Yellowstone National Park during June–September, 1995. *US Geol Surv Open-File Rep* 02-344.
- Fournier, R.O., D.E. White, and A.H. Truesdell. 1976. Convective heat flow in Yellowstone National Park. Proc 2nd UN Symp Development and Use of Geothermal Resources, San Francisco, 731–9.
- Gemery-Hill, P., W.C. Shanks, III, L.S. Balistreri, and G. Lee. In press, Geochemical Data for selected rivers, lake waters, hydrothermal vents and sub-aerial geysers in Yellowstone National Park, Wyoming, and vicinity, 1996–2002. In *Integrated Geoscience Studies in the Greater Yellowstone Area: Volcanic, Hydrothermal, and Tectonic Processes in the Yellowstone Geocosystem*, ed. L.A. Morgan. US Geol Surv Prof Pap.
- Good, J.M., and K.L. Pierce. 1996. *Interpreting the landscapes of Grand Teton and Yellowstone National Parks, Recent and ongoing geology*. Grand Teton National Park, WY: Grand Teton Natural History Association.
- Hamilton, W.L. 1987. Water level records used to evaluate deformation associated with the Yellowstone caldera. *J Volcanol Geotherm Res* 31:205–10.
- Hildreth, W., R.L. Christiansen, and J.R. O'Neil. 1984. Catastrophic isotopic modification of rhyolitic magma at times of caldera subsidence, Yellowstone Plateau volcanic field. *J Geophys Res* 89:8339–69.
- Johnson, S.Y., W.J. Stephenson, L.A. Morgan, W.C. Shanks, III, and K.L. Pierce. 2003. Hydrothermal and tectonic activity in northern Yellowstone Lake, Wyoming. *Geol Soc Am Bull* 115:954–71.
- Klump, J.V., C.C. Remsen, and J.L. Kaster. 1988. The presence and potential impact of geothermal activity on the chemistry and biology of Yellowstone Lake, Wyoming. In *Global venting, midwater and benthic ecological processes*, ed. M. DeLuca and I. Babb, 81–98. NOAA Symp Undersea Res 4.
- Lehman, J.A., R.B. Smith, and M.M. Schilly. 1982. Upper crustal structure of the Yellowstone caldera from seismic delay time analyses and gravity correlations. *J Geophys Res* 87:2713–30.
- Locke, W.W., and G.A. Meyer. 1994. A 12,000 year record of vertical deformation across the Yellowstone caldera margin—The shorelines of Yellowstone Lake. *J Geophys Res* 99:20079–94.
- Mason, B.G., D.M. Pyle, and C. Oppenheimer. 2004. The size and frequency of the largest explosive eruptions on Earth. *Bull Volcanol* 66:735–48.
- Meyer, G.A., and W.W. Locke. 1986. Origin and deformation of Holocene shoreline terraces, Yellowstone Lake, Wyoming. *Geology* 14:699–702.
- Morgan, L.A., W.C. Shanks, III, K.L. Pierce, D.A. Lovalvo, G. Lee, M. Webring, W.J. Stephenson, S.Y. Johnson, S. Harlan, B. Schulze, and C. Finn. In press, The floor of Yellowstone Lake is anything but quiet: New Discoveries from high-resolution sonar imaging, seismic-reflection profiles, and submersible studies. In *Integrated Geoscience Studies in the Greater Yellowstone Area: Volcanic, Hydrothermal, and Tectonic Processes in the Yellowstone Geocosystem*, ed. L.A. Morgan. US Geol Surv Prof Pap.

- Morgan, L.A., W.C. Shanks, III, D.A. Lovalvo, S.Y. Johnson, W. Stephenson, K.L. Pierce, S. Harlan, C. Finn, G. Lee, M. Webring, B. Schulze, J. Duhn, R. Sweeney, and L. Balistreri. 2003. Exploration and Discovery in Yellowstone Lake: Results from High-Resolution Sonar Imaging, Seismic Reflection Profiling, and Submersible Studies. *J Volcanol Geotherm Res* 2003:221-42.
- Morgan, L.A., W.C. Shanks, D. Lovalvo, S.Y. Johnson, W.J. Stephenson, S.S. Harlan, E.A. White, J. Waples, and J.V. Klump. 1999. New discoveries from the floor of Yellowstone Lake: Results from sonar imaging, seismic reflection, and magnetic surveys. *Geol Soc Am Abstract* 31:A-207.
- Morgan, L.A., W.C. Shanks, K.L. Pierce, and R.O. Rye. 1998. Hydrothermal explosion deposits in Yellowstone National Park—Links to hydrothermal processes. *EOS Trans AGU* (fall meeting) *Abstract* F964.
- Morgan, P., D.D. Blackwell, R.E. Spafford, and R.B. Smith. 1977. Heat flow measurements in Yellowstone Lake and the thermal structure of the Yellowstone caldera. *J Geophys Res* 82:3719-32.
- Muffler, L.J.P., D.E. White, and A.H. Truesdell. 1971. Hydrothermal explosion craters in Yellowstone National Park. *Geol Soc Am Bull* 82:723-40.
- Obradovich, J.D. 1992. Geochronology of the late Cenozoic volcanism of Yellowstone National Park and adjoining areas, Wyoming and Idaho. *US Geol Surv Open-File Rep* 92-408.
- Otis, R.M., R.B. Smith, and R.J. Wold. 1977. Geophysical surveys of Yellowstone Lake, Wyoming. *J Geophys Res* 82:3705-17.
- Pelton, J.R., and R.B. Smith. 1982. Contemporary vertical surface displacements in Yellowstone National Park. *J Geophys Res* 87:2745-51.
- Pierce, K.L. 1974. Surficial geologic map of the Tower Junction quadrangle and part of the Mount Wallace quadrangle, Yellowstone National Park, Wyoming and Montana. *US Geol Surv Misc Invest Series Map* I-647.
- Pierce, K.L. 1979. History and dynamics of glaciation in the northern Yellowstone National Park area. *US Geol Survey Prof Pap* 729-F.
- Pierce, K.L., K.P. Cannon, and G. Meyer. 1997. Yellowstone caldera “heavy breathing” based on Yellowstone Lake and River changes in post-glacial time. *EOS Trans AGU Abstract* 78:802.
- Pierce, K.L., K.P. Cannon, G.A. Meyer, M.J. Trebesch, and R. Watts. 2002. Post-glacial inflation-deflation cycles, tilting, and faulting in the Yellowstone caldera based on Yellowstone Lake shorelines. *US Geol Surv Open-File Rep* 02-142.
- Pierce, K.L., D.G. Despain, L.A. Morgan, and J.M. Good. In press. The Yellowstone hotspot, Greater Yellowstone Ecosystem, and Human Geography. In *Integrated Geoscience Studies in the Greater Yellowstone Area: Volcanic, Hydrothermal, and Tectonic Processes in the Yellowstone Geocosystem*, ed. L.A. Morgan. US Geol Surv Prof Pap.
- Remsen, C.C., J.V. Klump, J.L. Kaster, R. Paddock, P. Anderson, and J.S. Maki. 1990. Hydrothermal springs and gas fumaroles in Yellowstone Lake, Yellowstone National Park, Wyoming. *Nat Geo Res* 6:509-15.
- Richmond, G.M. 1973. Surficial geologic map of the West Thumb quadrangle, Yellowstone National Park, Wyoming. *US Geol Surv Misc Geologic Invest Map* I-643.
- Richmond, G.M. 1976. Surficial geologic history of the Canyon Village quadrangle, Yellowstone National Park, Wyoming. *US Geol Surv Bull* 1427.
- Richmond, G.M. 1977. Surficial geologic map of the Canyon Village quadrangle, Yellowstone National Park, Wyoming. *US Geol Surv Misc Invest Series Map* I-652.
- Rye, R.O., and A.H. Truesdell. 1993. The question of recharge to the geysers and hot springs of Yellowstone National Park. *US Geol Surv Open-File Rep* 93-384.
- Shanks, W.C., III, J. Alt, and L.A. Morgan. In press. Geochemistry of sublacustrine hydrothermal deposits in Yellowstone Lake: hydrothermal reactions, stable isotope systematics, sinter deposition, and spire growth. In *Integrated Geoscience Studies in the Greater Yellowstone Area: Volcanic, Hydrothermal, and Tectonic Processes in the Yellowstone Geocosystem*, ed. L.A. Morgan. US Geol Surv Prof Pap.
- Smith, R.B. 1991. Earthquake and geodetic surveillance of Yellowstone. *Seismol Res Lett* 62:27.
- Stanley, W.D., D.B. Hoover, M.L. Sorey, B.D. Rodriguez, and W.D. Heran. 1991. Electrical geophysical investigations in the Norris-Mammoth corridor, Yellowstone National Park, and the adjacent Corwin Springs Known Geothermal Resources Area. *US Geol Surv Water-Resources Inv* 91-4052:D1-18.
- Sturchio, N.C., M.T. Murrell, K.L. Pierce, and M.L. Sorey. 1992. Yellowstone travertines; U-series ages and isotope ratios (C, O, Sr, U). *Proc Int Symp Water Rock Interaction* 7:1427-30.
- Sturchio, N.C., K.L. Pierce, M.T. Murrell, and M.L. Sorey. 1994. Uranium-series ages of travertines and timing of the last glaciation in the northern Yellowstone area, Wyoming-Montana. *Quatern Res* 41:265-77.
- U.S. Geological Survey. 1972. Geologic map of Yellowstone National Park. *US Geol Surv Misc Invest Series Map* I-711.
- Waite, G.P., and R.B. Smith. 2002. Seismic evidence for fluid migration accompanying subsidence of the Yellowstone caldera. *J Geophys Res* 107:2177.
- Werner, C., S.L. Brantley, and K. Boomer. 2000. CO₂ emissions related to the Yellowstone volcanic system; 2, Statistical sampling, total degassing, and transport mechanisms. *J Geophys Res* 105:10831-46.
- Werner, C., and S. Brantley. 2004. CO₂ emissions from the Yellowstone volcanic system. *Geochem Geophys Geosyst* 4:1-26.

- Wicks, C.W., Jr., W.R. Thatcher, and D. Dzurisin. 1998. Migration of fluids beneath Yellowstone caldera inferred from satellite radar interferometry. *Science* 282:458–62.
- Wold, R.J., M.A. Mayhew, and R.B. Smith. 1977. Bathymetric and geophysical evidence for a hydrothermal explosion crater in Mary Bay, Yellowstone Lake, Wyoming. *J Geophys Res* 82:3733–8.